Methods of Depth Measurement and Image Fusion Based on Multi-focus Micro-images

Yin Ying-jie[1], Wang Xin-gang[1], Xu De[1], Zhang Zheng-tao[1], Bai Ming-ran[1], Shi Gang[2]
1. Research Center of Precision Sensing and Control, Institute of Automation, Chinese Academy of Sciences, Beijing 100190
E-mail: yingjie.yin@ia.ac.cn
2. Wuhan Railway Bureau, Wuhan 430070, China

Abstract: When a small object is measured by micro cameras, a sharp image of the whole object is impossible to be obtained because the depth of the object's surface is different and the distance between different parts of the object's surface maybe deeper than the depth of field of the micro camera. The camera is focused on different areas of the object's surface and a series of multi-focus images are taken. The relative depths between the object surface's different sub-regions will be got by comparing image sharpness evaluation function values of multi-focus images' same sub-regions and considering the relative position between the camera and the object. Thus the surface depth is obtained. Multi-focus images' sub-regions with maximum image sharpness evaluation function values are combined into an image. The experimental results verify the effectiveness of the proposed methods.

Key Words: depth of field; sharpness evaluation function; depth measurement; multi-focus; micro-image; image fusion

1 INTRODUCTION

Micro-images of the small object need to be processed when the object is measured under micro-vision. The depth of field (DOF) of the micro-camera is narrow, so a sharp image of the whole object can't be obtained by focusing the camera only one time. The problem can be solved by multi-focus images fusion methods. The methods usually focus the camera on different areas of the object's surface to obtain the multi-focus images under the same imaging condition. A sharp image of the whole object is formed by fusing the images. Burt and Adelson[1] propose the laplacian pyramid method, H.Li [2] proposes the method of using the wavelet transform to achieve the multi-sensor image fusion. Now, many new image fusion algorithms based on the wavelet transform [3-7] are proposed. These algorithms can accomplish the image fusion of multi-focus micro-images effectively, but methods of measuring the depth of objects aren't proposed. In order to solve this problem, methods of depth measurement and image fusion based on multi-focus micro-images are proposed. Images of the small object in different planes of focus are taken by the microscopic camera. The relative depths of the object surface's different sub-regions will be got by comparing image sharpness evaluation function (ISEF) values of multi-focus images' same sub-regions and considering the relative position between the camera and the object. Thus the surface depth is obtained. Multi-focus images' sub-regions with maximum ISEF value are fused into a sharp image. The experimental results show the methods can obtain the depth information of the object's surface effectively.

This work is supported by National Nature Science Foundation under Grant 61105036 and 61227804

2 DEPTH MEASUREMENT AND IMAGE FUSION BASED ON MULTI-FOCUS MICRO-IMAGES

2.1 Depth Measurement of Small Objects

The DOF of the micro-camera is narrow, and the DOF is associated with parameters of the camera. The imaging principle of the camera is shown in Fig.1, ΔL_1 is the distance between the front boundary of DOF and the focus, ΔL_2 is the distance between the back boundary of DOF and the focus, u is the distance between the focus and the lens, f is the focal length, δ is the diameter of permissible circle of confusion, D is the diameter of aperture, v is the image distance.

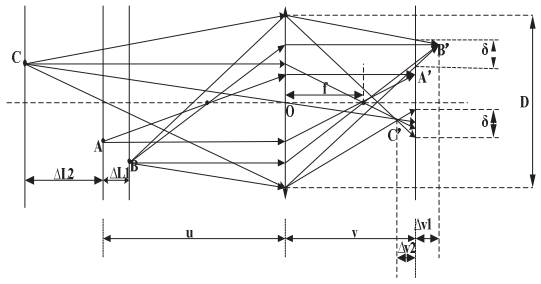

Fig 1. The imaging principle of the camera

The point A is in the focal plane, the point B is in the front boundary plane of the DOF, the point C is in the back boundary plane of the DOF.

To the point A, we have the formula (1):

$$\frac{1}{u}+\frac{1}{v}=\frac{1}{f} \tag{1}$$

To the point B, we have the formula (2):

$$\frac{1}{u\text{-}\Delta L_1}+\frac{1}{v+\Delta v_1}=\frac{1}{f} \tag{2}$$

978-1-4673-5534-6/13/$31.00 ©2013 IEEE

From the formula (2), ΔL_1 can be obtained as follows:

$$\Delta L_1 = \frac{(u-f)\Delta v_1}{(v+\Delta v_1-f)} \tag{3}$$

From the geometrical relationship in Fig.1, we have the formula (4):

$$\frac{\delta}{D} = \frac{\Delta v_1}{v+\Delta v_1} \tag{4}$$

From the formula (4), Δv_1 can be obtained as follows:

$$\Delta v_1 = \frac{\delta v}{D-\delta} \tag{5}$$

From the formula (1), the formula (3) and the formula (5), ΔL_1 can be obtained as follows:

$$\Delta L_1 = \frac{\delta F u(u-f)}{f^2+F\delta(u-f)} \tag{6}$$

To the point *C*, we have the formula (7):

$$\frac{1}{u+\Delta L_2} + \frac{1}{v-\Delta v_2} = \frac{1}{f} \tag{7}$$

From the formula (7), ΔL_2 can be obtained as follows:

$$\Delta L_2 = \frac{(u-f)\Delta v_2}{v-f-\Delta v_2} \tag{8}$$

From the geometrical relationship in Fig.1, we have the formula (9):

$$\frac{\delta}{D} = \frac{\Delta v_2}{v-\Delta v_2} \tag{9}$$

From the formula (1), the formula (8) and the formula (9), ΔL_2 can be obtained as follows:

$$\Delta L_2 = \frac{Fu\delta(u-f)}{f^2-F\delta(u-f)} \tag{10}$$

From the formula (6) and the formula (10), the DOF ΔL can be obtained as follows:

$$\begin{aligned}\Delta L &= \Delta L_1+\Delta L_2 = \frac{Fu\delta(u-f)}{f^2+F\delta(u-f)} + \frac{Fu\delta(u-f)}{f^2-F\delta(u-f)} \\ &= \frac{2Fu\delta f^2(u-f)}{f^4-F^2\delta^2(u-f)^2}\end{aligned} \tag{11}$$

In the formula (6), the formula (10) and the formula (11), F equals to f/D. The parameter u is const value when the parameters f, δ, D, ΔL are const values in the formula (11). Sub-regions of the object's surface will form sharp images in the image plane when the distance between the sub-regions and the camera's lens is equal to u. The DOF of the microscopic camera is narrow, so the distances between sub-regions of the object's surface and the camera's lens can be recognized as u when the sub-regions form sharp images in the image plane.

Lens of the microscopic camera and the stage remain parallel (the camera is usually right above the stage). Parameters of the camera stay unchanged when the depths of the object's surface is measured. The camera is adjusted away from the object until all the sub-regions of the object form blurred images in the image plane, and the camera's final position is as the start position of the camera to measure the object.

The object's image is saved in the initial position of the camera. Then the camera is moved towards the object along the optical axis direction with the same moving step length (the step length is near to the DOF) until all the sub-regions of the object form blurred images in the image plane. The object's images are saved when the camera is in different locations. Then a serials of images are obtained, and the serial number of an image corresponds to the distance between the object and the camera.

Each image is divided into m rows n columns sub-regions. The partitioning method is showed in Fig.2. $P_{i\,[k,\,j]}$ is the row k column j sub-region of the object's image which is taken when the camera moves i-1 steps towards the object along the optical axis direction. The ISEF values of all sub-regions of all images are calculated.

The serial numbers of the sub-regions with the maximal ISEF value are found by comparing the ISEF values of the same sub-regions of the different images. If $P_{i\,[k,\,j]}$ stands for a sub-region, the ISEF values of $P_{i\,[k,\,j]}$ with the same k and j but different i will be compared, then the serial number i corresponding to the maximal ISEF value will be found. The actual depth of any two sub-regions of the object's surface can be obtained when the serial number i corresponding to the maximal ISEF value and the camera's moving step length are known. For example, if the serial number i is equal to 15 when the ISEF value of $P_{i\,[1,\,2]}$ is maximal and the serial number i is equal to 8 when the ISEF value of $P_{i\,[1,\,9]}$ is maximal, the actual depth between the row 1 column 2 sub-region of the object's surface and the row 1 column 9 sub-region is $7\Delta z$ (Δz is the camera's moving step length).

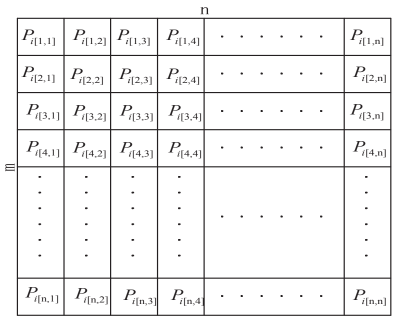

Fig 2. Sub-regions of the image

2.2 Sharpness Evaluation Function and Image Fusion

The ISEF is used to indicate the image sharpness. The sharper an image is, the larger the function value is. The ISEF value of sub-region image is largest when the distance between the sub-region of the object's surface and the camera's lens is equal to u. The sharpness evaluation methods include the gradient function method, the spectrum function method, the entropy function method and so on [8-10].

The Tenengrad function [11] of the gradient function is adopted as the sharpness evaluation function in the paper. The Sobel operators are used to calculate the gradient values in horizontal and vertical direction. The Tenengrad function $f(I)$ is defined as follows (T is a threshold):

$$f(I) = \sum_x \sum_y \left[S(x,y) \right]^2 \qquad \left(S(x,y) > T \right) \tag{12}$$

and

$$S(x,y) = \sqrt{G^2_x(x,y) + G^2_y(x,y)} \tag{13}$$

I is the image to be processed in the formula (12). $G_x(x, y)$ is the gradient value in horizontal direction, $G_y(x, y)$ is the gradient value in vertical direction in the formula (13).

The sub-regions of the images with the maximal ISEF value are combined into a sharp image.

3 EXPERIMENTS AND RESULTS

The Prosilica GC2450 camera produced by German Allied Vision Technologies Company is adopted in the experiment. An eraser with two planes is used as the measured object. A small piece of paper on which some characters are printed is stuck onto each plane of the eraser. The actual distance between the two planes is about 7.5mm.

Experimental procedure：

Step1: The eraser is put on the stage. The two planes of the easer are right above the camera. The microscopic camera's lens and the stage are parallelized. The camera is moved away from the eraser until all sub-regions of the eraser form blurred images in the image plane, and the camera's final position is as the start position of the camera to measure the eraser. The eraser's image is saved in the initial position of the camera. The camera is moved towards the eraser along the optical axis direction with the same moving step length （500um） until all sub-regions of the eraser form blurred images in the image plane. The eraser's images are saved when the camera is in different locations. The images are showed in Fig.3. The image corresponding to the initial position of the camera is showed in Fig.3(1), and the image corresponding to the final position of the camera is showed in Fig.3(27).

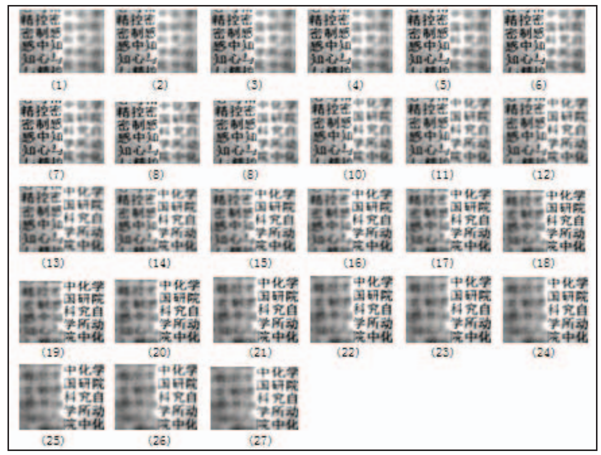

Fig 3. Images corresponding to the camera's different position

Step2: Each image is divided into18 rows 14 columns sub-regions. The sub-regions' ISEF values of all images are calculated according to the formula (12). The filter coefficients of the Sobel operator in the horizontal direction is [-1 0 1; -2 0 2; -1 0 1], and the filter coefficients of the Sobel operator in the vertical direction is [-1 -2 -1; 0 0 0; 1 2].

Step 3: The serial numbers of the sub-regions with the maximal ISEF value are found by comparing the ISEF values of the same sub-regions of different images. The results are shown in Table1. The actual depth of any two sub-regions of the eraser's surface can be obtained when the serial number corresponding to the maximal ISEF value and the camera's moving step length are known. The actual height of sub-region owning the maximal ISEF and the maximal serial number is set to zero, so the serial numbers of the sub-regions with the maximal ISEF value can be translated into the sub-regions' actual height. The results are shown in Table1. The eraser's three-dimensional graph shown in Fig.4 is drawn by using the data in Table1.

Table1. Actual Height of Sub-regions (mm)

column row	1	2	3	4	5	6	7
1	8.5	8.5	8.5	8.5	8.5	8.5	8.5
2	8.5	8.5	8.5	8.5	8.5	8.5	8.5
3	8.5	8.5	8.5	8.5	8.5	8.5	8.5
4	8.5	8.5	8.5	8.5	8.5	8.5	7.5

5	8.5	8.5	8.5	8.5	8.5	8.5	8.5
6	8.5	8.5	8.5	8.5	8.5	9	8.5
7	8.5	8.5	8.5	9	9	9	8.5
8	8.5	8.5	9	9	9	9	9
9	8.5	8.5	9	9	9	9	9
10	8.5	8.5	9	9	9	9	9
11	8.5	9	9	9	9	9	9
12	8.5	9	9	9	9	9	9
13	8.5	8.5	9	9	9	9	9
14	8.5	8.5	9	9	9	9	9
15	8.5	8.5	8.5	9	9	9	9
16	8.5	8.5	9	9	9	9	9
17	8	8.5	8.5	9	9	9	9
18	8	8.5	8.5	8.5	8.5	9	8.5

column row	8	9	10	11	12	13	14
1	1	1	1	0.5	0	1	1
2	2	1	1	0.5	1	1	1
3	3.5	0.5	1	1	1	1	0.5
4	4	0.5	1	0.5	0.5	0.5	0.5
5	2.5	1.5	1.5	1	1	1	1
6	1.5	1.5	1.5	1	1	1	1
7	1.5	1.5	1.5	1	1.5	1	1
8	3	2.5	1	1.5	1	1	0.5
9	2.5	1.5	1.5	1.5	1	1	1
10	2.5	1.5	1	1.5	1	1	1
11	1	1.5	1.5	1.5	1	1	0.5
12	2.5	1.5	1.5	1.5	1	1	0.5
13	1.5	1.5	1.5	1.5	1	1	1
14	1.5	1.5	1.5	1.5	1.5	1	0.5
15	1.5	1.5	1.5	1.5	1	1	1
16	1.5	1.5	1.5	1.5	1	1	0.5
17	1.5	1.5	1.5	1.5	1	1	0.5
18	1.5	1.5	1.5	1	1	0.5	1

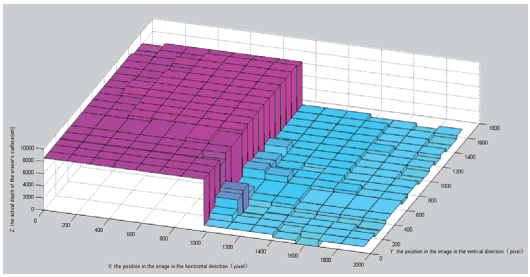

Fig 4. The 3-D Graph of the Eraser

Step5: Sub-regions of the eraser's image with the maximal ISEF value are combined into an image. The result is shown in Fig.5.

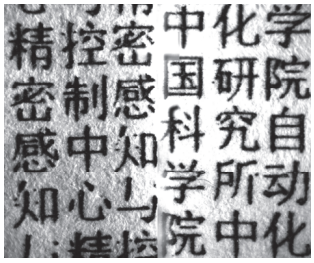

Fig 5. The result image of image fusion

The mean distance of the two planes of the eraser obtained from the experiments is 7.49mm, the error is about 0.01mm.

4 CONCLUSION

Methods of depth measurement and image fusion based on multi-focus micro-images are proposed. The character of the micro-camera's narrow DOF is creatively used to measure the depth of small objects' surface. The results of experiments suggest the methods have high accuracy in the depth measurement of the small object. The methods also have the important meaning for 3-D modeling of the small object.

REFERENCES

[1] P. J. Burt, E. H. Adelson. The laplacian pyramid as a compact image code[J], IEEE Transactions on Communication, 1883, 31(4): 532-540..

[2] H. Li. Multi-sensor image fusion using the wavelet transform[J], Graphical Models and Image Processing, 1995, 57(3): 235-245.

[3] Z. Jiang, D. Han, J. Chen, et al. A wavelet based algorithm for multi-focus micro-image fusion[A], Proceeding of the Third International Conference on Image and Graphics[C], Hong Kong, IEEE Computer Society Process, 2004, 176-179.

[4] X. L. Qun, Y. Zi, X. S. Cai, et al. Hong. A fast and easy fusion method for multi-focus micro-image[J], Optical Instruments, 2007, 29(5): 13-17.

[5] C. Gong, G. Lei, Z. T. Yun, et al. Multi-focus image fusion method based on wavelet transform[J], Computer Engineering and Applications, 2012, 48(1):194-196.

[6] X. Li, M. He, M. Roux. Multifocus image fusion based on redundant wavelet transform[J], IET Image Process, 2010, 4(4): 283-293.

[7] A. Abd-el-kader, H. E. Moustafa, S. Rehan. Performance Measures for Image Fusion Based on Wavelet Transform and Curvelet Transform, the 28th National Radio Science Conference, 2011.

[8] H. Harms, H. M. Aus. Comparison of digital focus criteria for a TV microscope system. Cytometry, 1984, 5: 236-243.

[9] F. C.A. Groen, I. T. Young, G. Ligthart. A comparison of different focus functions for use in autofocus algorithms, Cytometry, 1985, 6: 81-91.

[10] L. Firestone, K. Cook, K. Culp, N. Talsania, K. Preston. Comparison of autofocus methods for automated micros-copy, Cytometry, 1991, 12: 195-205.

[11] N. K. C. Nathaniel, P. A. Neow, M. H. A. Jr. Practical issues in pixel-based autofocusing for machine vision[A]. Proceedings of the 2001 IEEE International Conference on Robotics & Automation[C], Seoul, Korea. IEEE Robotics and Automation Society, 2001: 2791-2796.